Reprinted from JOURNAL OF THE ELECTROCHEMICAL SOCIETY
Vol. 128, No. 5, May 1981
Printed in U.S.A.

An Efficient Integration Technique for Use in the Multilayer Analysis of Spreading Resistance Profiles

H. L. Berkowitz* and R. A. Lux

U.S. Army Electronics Technology and Devices Laboratory, ERADCOM, Fort Monmouth, New Jersey 07703

ABSTRACT

The efficiency of multilayer analysis in calculating resistivity profiles from spreading resistance measurements depends on the rapid numerical evaluation of the well-known correction factor integral first introduced by Schumann and Gardner. We present a new approximate form for the correction factor which allows its numerical evaluation with only 22 integrand values for each evaluation of the integral. When this technique is used in our multilayer analysis program, we unfold spreading resistance profiles at the real time rate of less than 3 sec/point on a desktop computer. Its results match those of analytic evaluations of special two layer cases or with more elaborate numerical evaluations of graded structures to within 1%.

Two-probe spreading resistance measurement has become a widely used technique for determining impurity profiles in semiconductors (1-4). The conductivity of the material contacted by the probes is given by

$$R = C/(2a\sigma) \qquad [1]$$

where R is the measured spreading resistance, a is the contact radius, and C is a correction factor which is a function of the conductivity profile of the material. The multilayer analysis technique of evaluating this correction factor was originally proposed by Shumann and Gardner (1) and later developed in more easily calculated forms (2-4); complete derivations are given in Ref. (2, 3). In this technique the correction factor is

$$C = \frac{8}{I}\int_0^\infty dx \left[\frac{J_1(x)}{x} - \frac{J_0(Dx)}{2}\right] \underline{I}(x) F(tx) \qquad [2]$$

I is the total current flowing between the probes, where J_1 and J_0 are Bessel functions of the first kind, D and t are, respectively, the probe separation and layer thickness measured in probe radii, F (sometimes denoted by $1 + 2\Theta$) is a function of all conductivities deeper than the contacted layer, and $\underline{I}(x)$ is the Hankel transform of the normal component of the current density $I(r)$ at a probe. F can be expressed by a recursion relation

$$F_{i+1} = \frac{F_i\sigma_{i+1} + \sigma_i \tanh(tx)}{\sigma_i + F_i\sigma_{i+1}\tanh(tx)} \qquad [3]$$

which is equivalent to a form given by Choo (3). $\underline{I}(x)$ is given by

* Electrochemical Society Active Member.
Key words: resistivity profiles, spreading resistance measurements.

$$\underline{I}(x) = \int_0^a J_0(xr/a)I(r)rdr$$

Two forms of $\underline{I}(x)$ are found in the literature

$$\underline{I}(x) = \frac{I\sin(x)}{2\pi x} \quad [4]$$

which was first used by Shumann and Gardner (1) and

$$\underline{I}(x) = \frac{IJ_1(x)}{\pi x} \quad [5]$$

which was suggested by Severin (5) and used by Choo (6); the latter is used in the remainder of this paper. A complete discussion of the consequences of using either form is given in Ref. (7).

The calculation of a conductivity profile from a set of measured spreading resistances proceeds as follows. Starting at the deepest point, the value of the conductivity (and the resulting correction factor) is adjusted until the calculated spreading resistance agrees with the measured spreading resistance to the required accuracy. When this is achieved, the process is repeated at the next point, continuing until the entire set of measurements has been exhausted. The trial conductivity enters the calculation of the correction factor only through the function F. Hence during a numerical evaluation of C only the function F need be recalculated, the remainder of the integrand in Eq. [2] having been calculated once and stored as a numerical array.

Because the multilayer analysis scheme may require several evaluations of the correction factor per point an efficient technique for its evaluation is desirable. In this paper we introduce an approximation to the correction factor integral which can be evaluated rapidly. We then develop a numerical method which evaluates the approximate integral by sampling the integrand at only 22 points. We then compare this method with an analytic evaluation for special cases and with other numerical methods for a full multilayer case.

Approximation of the Correction Factor

The correction factor integral in Eq. [2] contains a term proportional to $J_0(Dx)/2$ which describes the voltage reduction at one probe due to the other probe. On physical grounds its effect can be significant only when the conductivity of the contacted layer is very high or when the spacing between probes is small, for which case Choo (3) showed that the primary effect of the J_0 term is to assure that the integrand vanishes at $x = 0$, even when F is singular at the origin.

In this section we show that it is possible to approximate the correction factor integral by an integral without a J_0 term by integrating from a nonzero lower limit

$$C_a = \frac{8}{\pi}\int_L^\infty dx\left(\frac{J_1(x)}{x}\right)^2 F(tx) \quad [6]$$

where L is given by

$$L = 2e^{-\gamma}/D \quad [7]$$

Here γ is Euler's constant, 0.577.... We demonstrate this by direct calculation of C and C_a in three cases which are amenable to analytic methods, namely (a) a conducting layer over an insulating substrate, (b) a conducting layer over a perfect conductor, and (c) a uniform semi-infinite slab. The appropriate forms of F are, respectively

$$F_A = \coth(tx), \quad F_B = \tanh(tx), \quad F_C = 1$$

For any multilayer case F must be within the envelope $\coth(tx)$ and $\tanh(tx)$. The test cases therefore represent the extreme cases and one intermediate case.

For thin conducting layers (i.e., in the limit $t \to 0$), the first two forms can be approximated by

$$F_A = 1/(tx), \quad F_B = tx$$

allowing the integral in Eq. [2] to be evaluated analytically. For case (a) the function F_A has a pole at $x = 0$; the lower limit L is chosen so as to minimize the difference between C and C_a for this case. Equation [2] written as

$$C = \frac{8}{\pi t}\lim_{\epsilon\to 0}\int_0^\infty \frac{J_1(x)}{x}\left[\frac{J_1(x)}{x} - \frac{J_0(Dx)}{2}\right]\frac{dx}{x^{1-\epsilon}}$$

a special case of the Weber Schafheitlin integral (8), yields

$$C = \frac{2}{\pi t}(\ln(D) + 1/4) \quad [8]$$

The corresponding value of C_a is obtained by evaluating Eq. [6]

$$C_a = \frac{8}{\pi t}\lim_{\epsilon\to 0}\left[\int_0^\infty \frac{J_1^2(x)}{x^{3-\epsilon}}dx - \int_0^L \frac{J_1^2(x)}{x^{3-\epsilon}}dx\right]$$

which yields

$$C_a = \frac{2}{\pi t}[\ln(2e^{-\gamma}/L) + 1/4 + L^2/8\ldots] \quad [9]$$

where γ is Euler's constant, 0.577....

With L set at

$$2e^{-\gamma}/D = 1.12292/D$$

the fractional difference between C and C_a in this case is minimized; its magnitude can be estimated by evaluating the term of order L^2, namely

$$\frac{C - C_a}{C} \approx 0.14/((\ln D + 0.25)D^2) \quad [10]$$

Using this value of L, both C and C_a were evaluated for cases (b) and (c); results are shown in Table I. These three cases represent very different physical situations. The fact that the errors introduced by using C_a rather than C are smaller than 1% when D is greater than 10 suggests that the approximation is generally useful: in most probe arrangements D is greater than 30. The numerical procedure for evaluating C_a is much simpler than that necessary to evaluate C. The latter involves calculating the integrand at enough points to follow the rapid oscillations of the function $J_0(Dx)$. For example, when D is equal to 30, $J_0(Dx)$ has more than 30 zeros at values less than the first zero of $J_1(x)$.

The Numerical Integrator

In this section we describe a numerical integrator which has been tailored to take advantage of the properties of the integrand of [6] in order to minimize the required evaluations of F.

Our objective is to choose a set of numbers x_i and weights w_i such that C_a can be well represented by a numerical approximation.

$$C_a = \Sigma\, w_i F(tx_i) \quad [11]$$

The appropriate numerical integration technique was selected so as to accommodate the most singular case, $F = \coth(tx)$ taking care that other cases were treated with sufficient accuracy.

Based on properties of $(J_1/x)^2$, we divide the domain of integration into four regions

(A) $L \leq x \leq 0.1$

(B) $0.1 \leq x \leq 1$

(C) $1 \leq x \leq j_{1,1}$

(D) $j_{1,1} < x$

where $j_{1,i}$ is the ith zero of the Bessel function J_1 and $j_{1,0} = 0$, $j_{1,1} = 3.83171$. In cases of practical significance

Table I. Functional forms of correction factors with $L = 1.12292/D$

F	C	C_a	$\lvert 1 - C_a/C \rvert$
$1/xt$	$\frac{2}{\pi t}(\ln D + 0.25)$	$\frac{2}{\pi t}\left(\ln D + 0.25 + \frac{L^2}{8} + \ldots\right)$	$\frac{0.14}{D^2(\ln D + 0.25)}$
1	$\frac{8}{\pi}\left(\frac{4}{3\pi} - \frac{1}{4D}\left(1 + \frac{1}{8D^2} + \ldots\right)\right)$	$\frac{8}{\pi}\left(\frac{4}{3\pi} - \frac{L}{4}\right)$	$0.072/D$
xt	$4t/\pi$	$t(4 - L^2)/\pi$	$0.03/D^2$

L is restricted to the domain $0.001 \leq L \leq 0.1$. In each region we choose a numerical integrator which will assure adequate convergence of the integrals.

In region (A) we replace $(J_1/x)^2$ by 1/4. In this region the most difficult integrand that can arise will be proportional to coth (tx), which approaches $1/(tx)$ for small x. To treat the pole at $x = 0$, we choose $\ln x$ to be the integration variable; this segment of C_a is then

$$\frac{8}{\pi}\int_{x=L}^{x=0.1} \frac{x}{4} F(tx)\, d(\ln x)$$

We then apply a nine point Newton-Cotes integrator to the integrand. The nine points, equally spaced in $\ln x$, are given by

$$x_i = L\,(0.1/L)^{(i/8)}, \quad 0 \leq i \leq 8$$

This segment of C_n is

$$\frac{1}{4\pi}\ln(0.1/L)\sum_0^8 w_{9,i} x_i F(tx_i) \qquad [12]$$

The weights $w_{9,i}$ for a nine point Newton-Cotes integrator are given in Ref. (9).

In region (B) the slowly varying $(J_1/x)^2$ is explicitly calculated. Again the most difficult integrand is proportional to $1/(tx)$, and we make the same transformation as in region (A). To achieve the same density of points in (B) as in (A), with $L = 0.001$, we use a five-point Newton-Cotes integration formula. This segment of C_n is then

$$\frac{2}{\pi}\ln(10)\sum_0^4 J_1^2(x_i) F(x_i)\, w_{5,i}/x_i \qquad [13]$$

The weights $w_{5,i}$ are given in Ref. (9) and $x_i = 0.1(10)^{(i/4)}$.

In region (C), $(J_1/x)^2$ is falling rapidly; a five-point Newton-Cotes integrator in x rather than $\ln x$ provides adequate coverage. This segment of C_n is

$$\frac{2}{\pi}(j_{1,1} - 1)\sum_0^5 (J_1(x_i)/x_i)^2 F(x_i) w_{5,i} \qquad [14]$$

Only four of the five points need be calculated, as $J_1(j_{1,1})$ is by definition zero.

In region (D), the rapid decrease in $(J_1/x)^2$ guarantees that the integral beyond the first zero, $j_{1,1}$, will make only a small contribution to the correction factor.

Using the mean value theorem

$$\int_{x=a}^{x=b} F(x)\, du(x) = F(\xi)\,(u(b) - u(a)) \qquad [15]$$

where $a \leq \xi \leq b$ and $du = (J_1/x)^2 dx$, we approximate the integral between successive zeros of J_1 by choosing ξ to be the centroid of $(J_1/x)^2$ between zeros

$$\xi = \frac{\int_a^b J_1^2(x)\,dx/x}{\int_a^b (J_1(x)/x)^2 dx} \qquad [16]$$

The approximation is exact if F varies at most linearly with x. We took five subintervals between successive zeros of J_1 to $j_{1,6}$, $x = 19.616$, and found that the integral truncated at this point was adequate for most integrands. [Albers (10) truncates at $x = 20$ and Choo (6) truncates at $x = 20.8$.] However, in cases where F is small in region (A) (for example when $F = \tanh(tx)$), an error of as much as 4% can be made due to this truncation. By using one additional point at the centroid of $(J_1/x)^2$ taken between 19.616 and infinity, this error can be reduced to below 1%.

This segment of C_n is then

$$\frac{8}{\pi}\sum w_{D,i} F(\xi_i) \qquad [17]$$

where the weights $w_{D,i}$ and ξ_i are shown in Table II. As the points at the region boundaries need be calculated only once, the complete integration requires only 22 evaluations of F.

Testing Procedures

The integration technique has been tested in the range $0.001 \leq t \leq 1$ and $10 \leq D \leq 1000$ for two layer cases where analytic results can be obtained and for representative multilayer distributions. We present the results of the two layer calculation and a sample multilayer case.

Test 1.—In the first test we compared C_n calculated using the 22 point integrator with C_a calculated analytically in the section Approximation of the Correction Factor.

$F(x)$ is replaced by tx, 1, and $1/(tx)$ in the cases now under consideration.

We evaluated C_n at 12 values of D between $D = 10$ and $D = 1000$ and list the maximum deviations in Table III. Maximum errors were found on comparing C with C_a and C_a with C_n. In all cases the maximum error occurs at $D = 10$.

In all cases we find agreement between the approximation and the numerical integrator to be better than 0.3%.

Table II. Centroids and weights used in region (D)

i	$a = j_{1,i}$	$b = j_{1,i+1}$	Centroid ξ_i	Weight $w_{D,i}$
1	3.83171	7.01558	5.23853	0.688546E-2
2	7.01558	10.1735	8.48093	0.163592E-2
3	10.1735	13.3237	11.6681	0.627777E-3
4	14.3237	16.4706	14.829	0.305139E-3
5	16.4706	19.6159	17.9661	0.173318E-3
6	19.6159	∞	39.3	0.4119E-3

Table III. Maximum deviations

F	$\lvert C - C_a \rvert / C$	$\lvert C_a - C_n \rvert / C_a$
tx	0.003	0.002
1	0.007	0.0006
$1/tx$	0.0006	0.0009

Test 2.—To measure the performance of our 22 point integrator for cases where analytic techniques were unavailable we constructed a Simpson integrator of 1597 points constructed as shown in Table IV.

This integrator was programmed in three versions to accommodate the various tests needed:

SIM which numerically integrates

$$\text{SIM} = \frac{8}{\pi}\int_0^{20}\left(\frac{J_1(x)}{x} - \frac{J_0(Dx)}{2}\right)\frac{J_1(x)}{x}F\,dx$$

SIMSG which evaluates the Schumann and Gardner correction factor

$$\text{SIMSG} = \frac{4}{\pi}\int_0^{20}\left(\frac{J_1(x)}{x} - \frac{J_0(Dx)}{2}\right)\frac{\sin(x)}{x}F\,dx$$

SIMT which corrects SIM for truncation error as described in the section The Numerical Integrator.

Truncating the integral at $x = 20$ allows us to compare our results with those of Albers (10), who generated spreading resistance data (*MD* in Table V) from model resistivity profiles by using the integration scheme of D'Avanzo *et al.* (4) over the interval $0 \leq x \leq 20$. Table V and Fig. 1 show one such data set calculated to represent the conductivity profile of a silicon wafer containing a Gaussian implant. Simulated spreading resistances were calculated from these conductivities for the case $a = 2$ μm, $D = 25$, $t = 0.015$ using SIMSG. We compared these to the set of resistances supplied by Albers. The largest fractional deviation found between the two data sets was less than 2 parts in 10^4. Spreading resistances were then calculated for the same data using the 22 point integrator, SIM, and SIMT. We find that agreement between the 22 point integrator and SIMT to be better than 5 parts in 10^3. This represents the total deviation between C and C_n for this case. A comparison between SIM and SIMT results indicate that the maximum relative deviation due to truncating at $x = 20$ for this case is about 2%.

Table IV. The 1597 point integrator

x, min.	x, max	Weights	Number of points
0	0.001	Trapezoidal	2
0.01	0.01	Simpson	199
0.01	0.1	Simpson	199
0.1	1	Simpson	199
1	20	Simpson	999

Table V. Summary of results calculating resistance as a function of depth in a layered medium using the various integrators mentioned in text. All calculations are based on the conductivity profile plotted in Fig. 1 and excerpted in this table for the case $a = 2$ μm, $D = 25$, $t = 0.015$.

A. Comparison of our large Simpson integrators SIM and SIMSG with the integration scheme of D'Avanzo

A.

Alber's model data				
Layer No.	Conductivity (mho-cm)	MD spreading resistance (Ω)	Fractional deviation 1-SIMSG/MD	Fractional deviation 1-SIM/MD
1	7.975E−03	1.744E+04	1.121E−05	−1.153E−01
4	1.940E−02	3.420E+03	1.144E−05	−1.054E−01
7	7.050E−01	3.895E+02	1.310E−04	−4.691E−02
10	9.775E+00	3.044E+02	1.780E−04	−2.769E−02
13	4.000E+01	3.101E+02	1.740E−04	−2.534E−02
16	1.010E+02	3.630E+02	1.924E−04	−2.478E−02
19	1.351E+02	5.639E+02	1.186E−04	−2.475E−02
22	8.547E+01	1.331E+03	9.739E−05	−2.487E−02
25	3.040E+01	4.756E+03	1.051E−04	−2.557E−02
28	6.203E+00	2.737E+04	5.895E−05	−2.982E−02
31	3.110E−01	1.840E+05	5.066E−06	−5.994E−02
34	1.177E−03	3.022E+06	−2.861E−06	−8.439E−02
37	7.926E−03	3.072E+06	−9.537E−06	−8.499E−02
40	7.908E−03	3.072E+06	−2.289E−05	−8.501E−02

B. Comparison of the results of our 22 point integrator and the Gauss Laguerre integrator with SIMT and SIM, respectively

B.

Layer No.	SIMT-OHMS	1-SIM/SIMT	Fractional deviation 1-(22)/SIMT	Fractional deviation 1-GL/SIM
1	1.976E+04	1.568E−02	2.388E−03	−6.939E−02
4	3.871E+03	2.332E−02	2.225E−03	−6.798E−02
7	4.103E+02	6.247E−03	3.481E−04	−4.640E−02
10	3.130E+02	6.092E−04	−1.259E−03	−3.891E−02
13	3.180E+02	1.796E−04	−1.380E−03	−3.802E−02
16	3.720E+02	6.694E−05	−1.457E−03	−3.782E−02
19	5.779E+02	3.421E−05	−1.642E−03	−3.781E−02
22	1.364E+03	2.933E−05	−2.220E−03	−3.796E−02
25	4.878E+03	2.241E−05	−3.438E−03	−3.874E−02
28	2.819E+04	1.830E−05	−7.906E−04	−4.469E−02
31	1.951E+05	6.187E−05	4.389E−03	−6.807E−02
34	3.279E+06	7.526E−04	3.595E−03	−7.096E−02
37	3.396E+06	9.924E−04	3.570E−03	−7.095E−02
40	3.396E+06	9.963E−04	3.573E−03	−7.095E−02

The Gauss Laguerre Integrator

To demonstrate the value of the lower limit cutoff approximation, we repeated the tests performed on the 22 point integrator using another sparse point numerical integrator the Gauss Laguerre integrator (GL in Table V) of Choo *et al.* (11). This integrator retains the term in $J_0(Dx)$.

In Fig. 2 we plot the fractional deviation between C and the Gauss Laguerre integrated correction factors in the cases of the section Testing Procedures, Test 1.

We find that the deviations for these cases tend to cluster in a band of ± 5% with occasional excursions to 10% or 20%. This is due principally to the fact that for D greater than 10, $J_0(Dx)$ has more than 60 zeros in the interval of $0 \leq x \leq 20$. The 33 points used for the GL integrator cannot hope to cover it adequately.

Discussion and Conclusions

We have presented a new approximate form for the correction factor integral of Schumann and Gardner which facilitates the rapid and accurate evaluation of

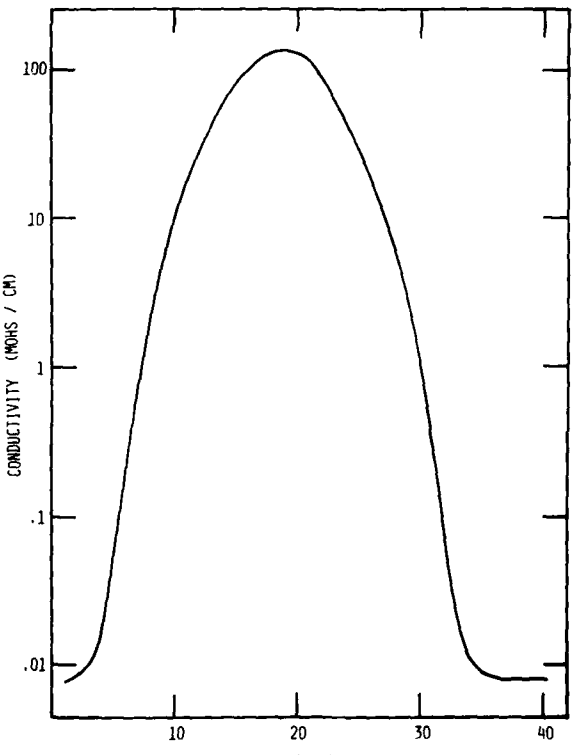

Fig. 1. Displays data supplied to us by Albers (10)

Fig. 1A. Plot of conductivity *vs.* depth for a model Gaussian implant.

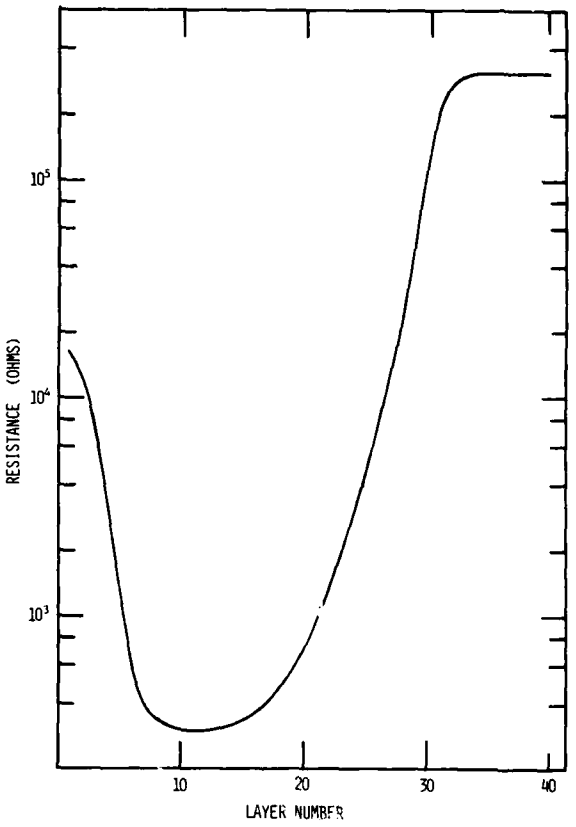

Fig. 1B. Plot of spreading vs. depth calculated by Albers using the integration scheme of D'Avanzo (4). The set shown here was calculated for $a = 2$ μm, $D = 25$, $t = 0.015$.

spreading resistance correction factors. This has been accomplished by eliminating the rapidly varying $J_0(Dx)$ term from the usual correction factor integral, Eq. [2].

Although we have presented the approximate integral of Eq [2] only for $\underline{I}(x)$ satisfying

$$\underline{I}(x) = \frac{IJ_1(x)}{\pi x}$$

the approximation remains valid with the lower limit, L, given by Eq. [7] for all current density profiles whose Hankel transform satisfies Eq. [4b] of (5)

$$\underline{I}(x) = \frac{I\,\Gamma(\nu+1)J_\nu(x)}{2\pi(x/2)^\nu}$$

All of the commonly used forms of $\underline{I}(x)$ are special cases of the above.

The integrator of the section The Numerical Integrator was incorporated into a multilayer analysis program described elsewhere (12). The program was written in BASIC for an HP system 9845. The time to calculate one point was generally less than 3 sec. As the time to measure a spreading resistance on modern equipment (*e.g.*, an ASR-100 probe) is about 6 sec the complete conductivity profile can be corrected as measurements are made.

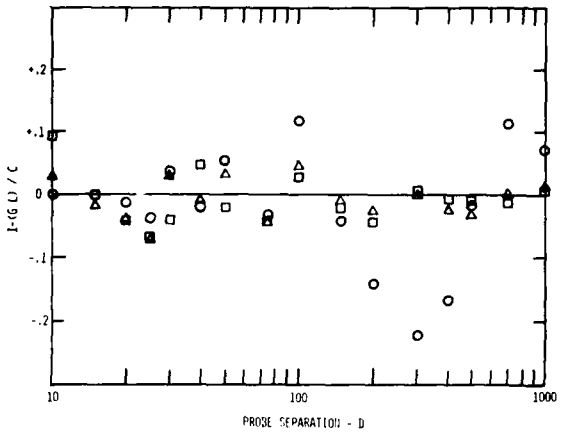

Fig. 2. Correction factors, GL, were calculated using the Gauss Laguerre integrator (11) for the Shumann and Gardner function, F, replaced by tx, 1, $1/tx$ and $10 \leq D \leq 1000$. Figure 2 shows a plot of the fractional deviation of GL from the analytically calculated correction factors, C of Table I. The squares, triangles, and circles refer to cases where F is set equal to tx, 1, $1/(tx)$, respectively.

Manuscript submitted April 14, 1980; revised manuscript received Nov. 6, 1980.

Any discussion of this paper will appear in a Discussion Section to be published in the December 1981 JOURNAL. All discussions for the December 1981 Discussion Section should be submitted by Aug. 1, 1981.

Publication costs of this article were assisted by the U.S. Army Electronics Technology and Devices Laboratory (ERADCOM).

REFERENCES

1. P. A. Schumann and E. E. Gardner, *Solid State Electron.*, **12**, 371 (1969).
2. Y. Iida, H. Abe, and M. Kondo, *This Journal*, **124**, 1118 (1977).
3. S. C. Choo, M. S. Leong, H. L. Hong, L. Li, and L. S. Tan, *Solid State Electron.*, **20**, 839 (1977).
4. D. C. D'Avanzo, R. D. Rung, A. Gat, and R. W. Dutton, *This Journal*, **125**, 1170 (1978).
5. P. J. Severin, Spreading Resistance Symposium, NBS. Special Publication 400-10, p. 27 (1974).
6. S. C. Choo, M. S. Leong, H. L. Hong, L. Li, and L. S. Tan, *Solid State Electron.*, **21**, 769 (1978).
7. H. L. Berkowitz and R. A. Lux, *This Journal*, **126**, 1479 (1979).
8. M. Abramowitz and I. A. Stegun, Editors, "Handbook of Math. Functions," NBS Applied Math Series 50, Third printing (1965), see Chap. II especially Eq. 11.4.34.
9. M. Abramowitz and I. A. Stegun, Editors, *ibid.*, Chap. 25, Eq. 25.4.14 and Eq. 25.4.18.
10. J. Albers, To be published in *Solid State Electron.*
11. S. C. Choo and M. S. Leong, *ibid.*, **22**, 405 (1979).
12. H. L. Berkowitz and R. A. Lux, To be published.